

## 35. OPHIOLITIC ROCKS OF THE MIDDLE AMERICA TRENCH LANDWARD SLOPE OFF GUATEMALA: DEFORMATIONAL CHARACTERISTICS AND TECTONIC SIGNIFICANCE<sup>1</sup>

Yujiro Ogawa, Department of Geology, Kyushu University  
Kantaro Fujioka, Ocean Research Institute, University of Tokyo  
and

Tadao Nishiyama, Seiichiro Uehara, and Masaharu Nakagawa, Department of Geology, Kyushu University<sup>2</sup>

### ABSTRACT

Dismembered ophiolitic rocks including abundant sheared, serpentinized peridotite (mostly harzburgite) and minor basalts, dolerites, gabbros, and altered metabasites (mainly altered amphibolite) were drilled at most of the sites on the upper to lower Middle America Trench landward slope off Guatemala during Leg 84 of the Deep Sea Drilling Project. These rocks show characteristic cataclastic deformation with zeolite facies metamorphism and alteration after amphibolite and greenschist facies metamorphism. These features indicate that the rocks originated in mid-oceanic ridge, off-ridge, and possibly other areas including island arc areas and were metamorphosed under a high geothermal gradient at low pressure. They were then structurally deformed and mixed within a serpentinite mélange. Such ophiolite mélanges may have been emplaced onto the Trench landward slope area during the initiation of subduction of the Cocos Plate. The emplacement seems to be connected to that of the Nicoya Complex in Costa Rica. The slope cover from early Eocene to Recent shows no history of these metamorphic and deformational events, therefore the emplacement of the dismembered ophiolitic rocks occurred at least before the early Eocene. The dismembered ophiolite-based Trench landward slope off Guatemala is a newly documented style of subduction, which has also recently been found at the easternmost edge of the Philippine Sea Plate along the Izu-Mariana-Yap Trench landward slope.

### INTRODUCTION

On Leg 67 a small amount of highly altered basaltic or intermediate igneous rock was recovered at Site 494, at the foot of the lower Trench slope off Guatemala (Aubouin, von Huene, Azéma, et al., 1982). But the abundant recovery of such materials on Leg 84 was unexpected before ophiolitic rocks were actually obtained on this Leg from almost the same sites as those of Leg 67 (Figs. 1 and 2). The ophiolitic rocks are composed mostly of serpentinized harzburgite at Site 570, serpentinized lherzolite at Site 566, and altered amphibolite at Site 569, whereas other lithologies such as basalt, dolerite, and gabbro were drilled together with serpentinized harzburgite at Site 567. Thus the rock assemblages vary from site to site, but as a whole may form a single body comprising a large mass of protruded dismembered ophiolite — an ophiolite mélange. The whole Trench landward slope is probably underlain by this dismembered ophiolite mass (Aubouin, von Huene, Baltuck, et al., 1982).

In this chapter we describe these rocks, specifically focusing on their deformation, metamorphism, and alteration. We present analytical data on minerals relevant to the discussion of the tectonic significance of these rocks.

### PROCEDURE

We collected samples of several different rock types from each site and focused our study on deformational features and related meta-

morphism and alteration. Thin sections of these samples were studied using a polarizing microscope to determine the mineral assemblages, textures, structures, and deformational and metamorphic characteristics. Some minerals were studied by X-ray diffraction (XRD) at Kyushu University, Japan, and others by using a Cambridge Instruments Microscan Electron Microprobe at Imperial College, U.K. In this case, the V probe was fitted with a Link EDS detector. The probe was operated at an accelerating voltage of 15 kV, a specimen current of 0.01  $\mu$ A, and a counting time of 100 s. For most of the analyses reported here, the beam was defocussed to 40  $\mu$ m to reduce decomposition, following the discussion of Morrison and Thompson (1983).

### DESCRIPTION OF DEFORMATIONAL CHARACTERISTICS OF THE OPHIOLITIC ROCKS

#### Site 566

Site 566 is located within the San José Canyon near the northern edge of the lower Trench slope area at about 3674 to 3865 m depth, where basement rocks were expected at a shallow depth with only a thin sedimentary cover. Serpentinite was first drilled at depths of only 21.9 and 88.1 m sub-bottom in Holes 566 and 566C, respectively, and the drilling penetrated 33.9 and 48.5 m of serpentinite, respectively. In Hole 566A, the first core penetrated 7 m sub-bottom and contained serpentinized lherzolite. Most of the ultramafic rocks are fully or considerably serpentinized, so that the densities are less than 3.0. The density values are listed in Figure 3, including those from Sites 566, 567, and 570. According to the rough measurements of two thin sections from Holes 566 and 566C, the rocks were originally lherzolite with the following composition: olivine—77%, orthopyroxene—11%, and clinopyroxene—12% with chrome spinel—3% (Sample 566-9-1, 7–9 cm, 52.8 m sub-bottom); and olivine—78%, orthopyroxene—10%, and clinopyroxene—12%

<sup>1</sup> von Huene, R., Aubouin, J., et al., *Init. Repts. DSDP*, 84: Washington (U.S. Govt. Printing Office).

<sup>2</sup> Addresses: (Ogawa, Nishiyama, Uehara, and Nakagawa) Department of Geology, Kyushu University 33, Hakozaki, Fukuoka 812, Japan; (Fujioka) Ocean Research Institute, University of Tokyo, Minamidai, Nakano, Tokyo 164, Japan.

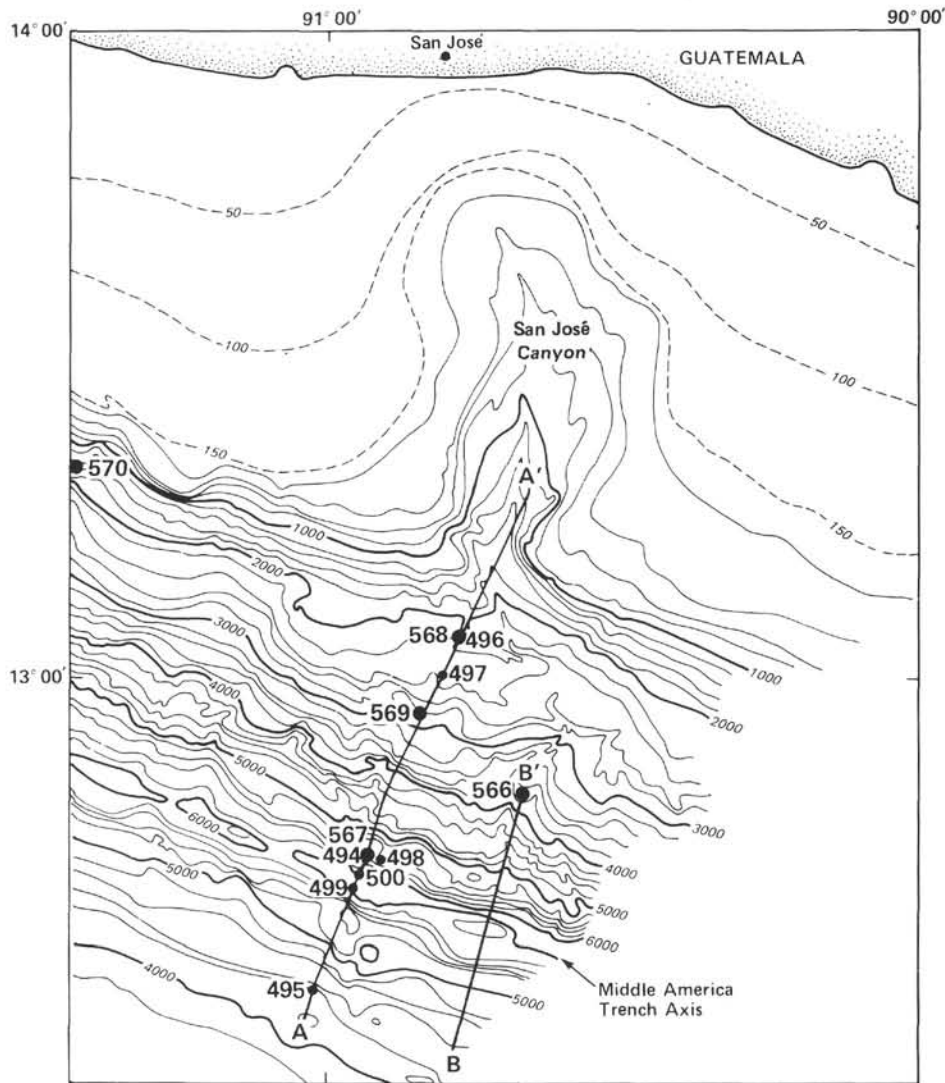


Figure 1. Map showing Leg 84 sites off Guatemala.

with a trace of chrome spinel (Sample 566C-5-1, 5-7 cm, 110.9 m sub-bottom) (Fig. 4). Most of the olivine and pyroxene has been serpentinized, forming chrysotile and lizardite of mesh and bastite textures, but the original minerals are arranged in a roughly foliated fashion. These rocks are probably cumulative peridotites showing later shearing. Sedimentary cover in the three holes varies, although they are only 1 km apart. Upper Pleistocene sediments (21.9 m thick) occur in Hole 566, Pliocene sediments (less than 7 m thick) in Hole 566A, and Miocene to Pleistocene sediments (88.1 m thick) lacking Pliocene deposits in Hole 566C. This indicates that the cover sediments are differently distributed and contain sedimentary hiatuses. The sediments contain no ophiolitic fragments (see lithology section, Site 566 report, this volume) and are composed only of sandy to muddy terrigenous materials. The canyon has thus been an area of variable sedimentation and erosion.

#### Site 567

Site 567 is located very near Site 494 of Leg 67, on the small bench at the very foot of the lower Trench

slope, just 3 km landward of the slope edge, 550 m above the Trench floor. Hole 567A penetrated ophiolitic rocks at several horizons. Thin layers made of serpentinite pebbles are included within the lower Miocene mudstone sections at 262.7 m sub-bottom. Other blue gray mud may be derived from altered serpentinite. In between 325.1 to 358.7 m rather thick sections of serpentinitic mud are intercalated. The sections show no sedimentary structures, and it is possible that these are tectonically emplaced as sheared clastite. However, just below the sections, Miocene fossils were found within terrigenous mudstone (see the lithology section, Site 567 report, this volume), so that these sections of serpentinitic mud are probably emplaced by tectonic processes.

Below 17.7 m of Campanian to Maestrichtian pelagic limestone, which was probably slumped or tectonically emplaced at this site, a 124.4-m-thick section of disrupted ophiolitic rock was penetrated. The recovery rate was very poor, averaging 9%, because hard basaltic to gabbroic rocks were encountered within sheared soft ophiolitic rocks. However, the variation of the drilling rate suggests an order of lithology as shown in Figure 5. The

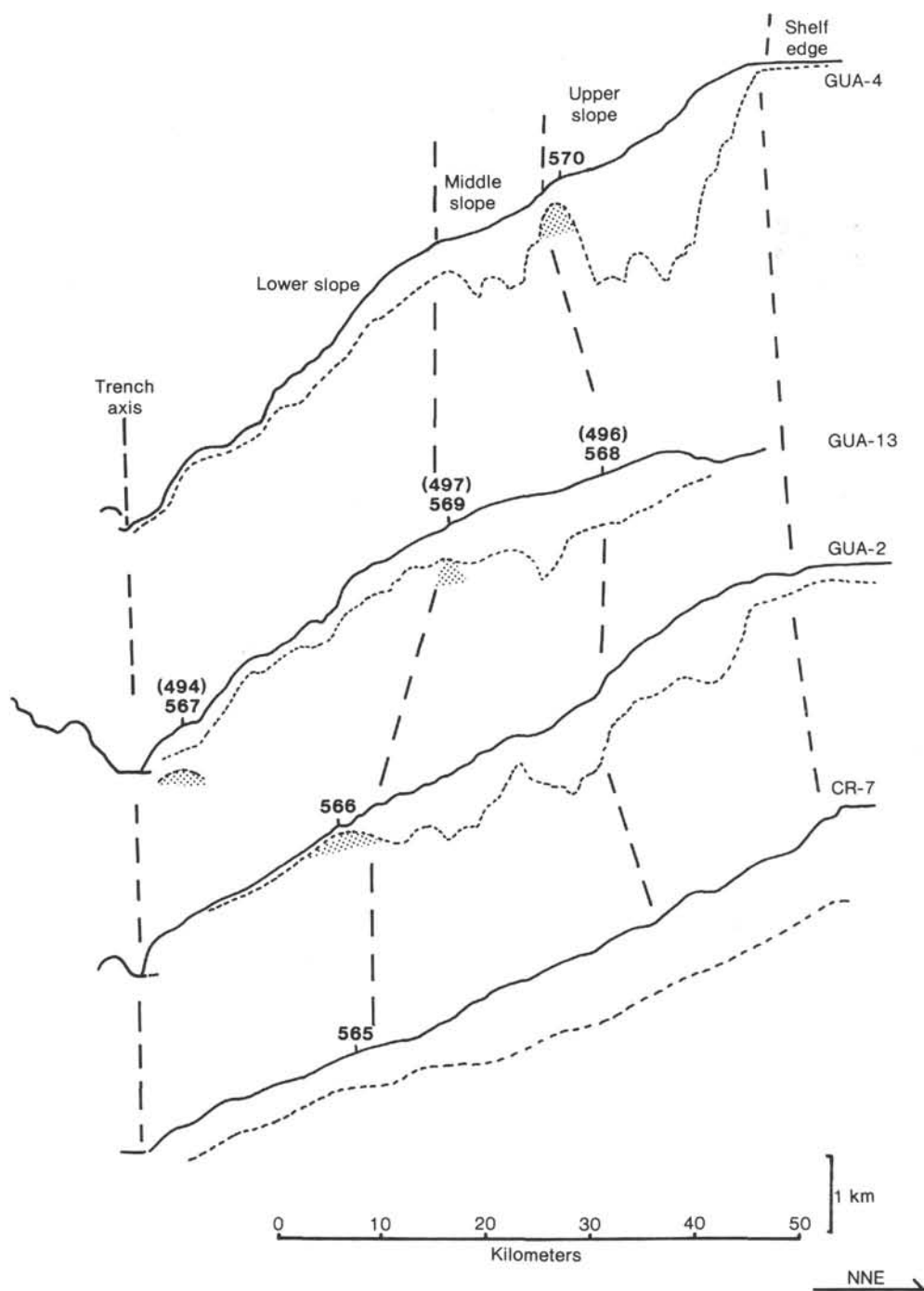


Figure 2. Schematic cross sections including Leg 84 sites off Guatemala and off Costa Rica. Drilled ophiolitic rocks are shown by shading. Vertical exaggeration =  $\times 13$ .

foliations observed in some sections of sheared serpentinite dip about 20 to 30°, as shown in Figure 5. The recovered rocks are quite disordered when compared to the commonly observed layered ophiolite sequence on-land of tectonized harzburgite, layered cumulate, high level intrusives, doleritic sheet dyke complex, basaltic volcanics, and sometimes pelagic sediment covers (Gass and Smewing, 1981). On Leg 84, no pelagic sedimentary rocks were recovered except for the possible pelagic mi-

critic Late Cretaceous limestone just above the ophiolitic rocks and umberlike metallic sediments in the crust of pillow lava described later. Thus, as far as we have observed in the cored section, rocks are very randomly intermixed tectonically within a serpentinite matrix, which is very sheared and pulverized. All the rocks characteristically show several stages of metamorphism, alteration, and deformation. The following sections describe general characteristics of deformation and mineralization.

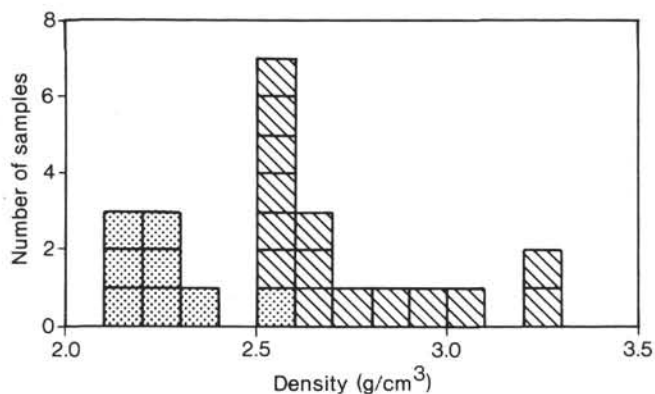


Figure 3. Distribution of the values of dry (dotted) and wet (cross-hatched) densities of serpentinite from Sites 566, 567, and 570. Those in the form of powder, sand, and mud were only measured in the dry state. These were placed in a drying oven for 42 hr. at 80°C. Rock fragments were measured wet after 24-hr. immersion in water.

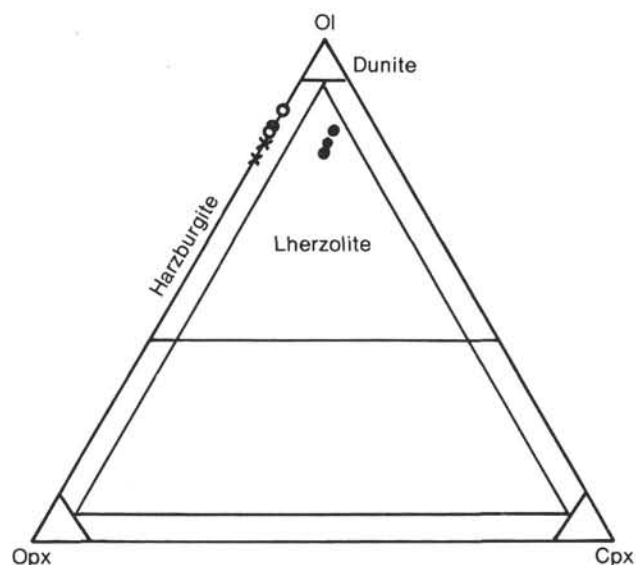


Figure 4. Olivine-orthopyroxene-clinopyroxene triangle diagram of peridotites. Closed circle = Site 566, open circle = Site 567, cross = Site 570.

**Sample 567A-20-1 (Piece 1, 103–106 cm)  
(369.4 m sub-bottom)**

This is an olivine-clinopyroxene gabbro. Olivine comprises about 15% content by volume and is partly chloritized. Clay is developed along the rim of olivine. Veins characterized by cataclasis of pyroxene, chloritized olivine, and plagioclase cut the rocks, and a part of the vein is further replaced by zeolite (analcite) (Fig. 6A). Such a cataclasis characterizes the entire section, but the gabbroic texture is still visible. Cataclasis followed chloritization but occurred before zeolite vein intrusion. Chlorite is developed from the wall of the vein and pulverized within the vein. Some part of the grain boundary are characterized by this type of cataclasis, but some

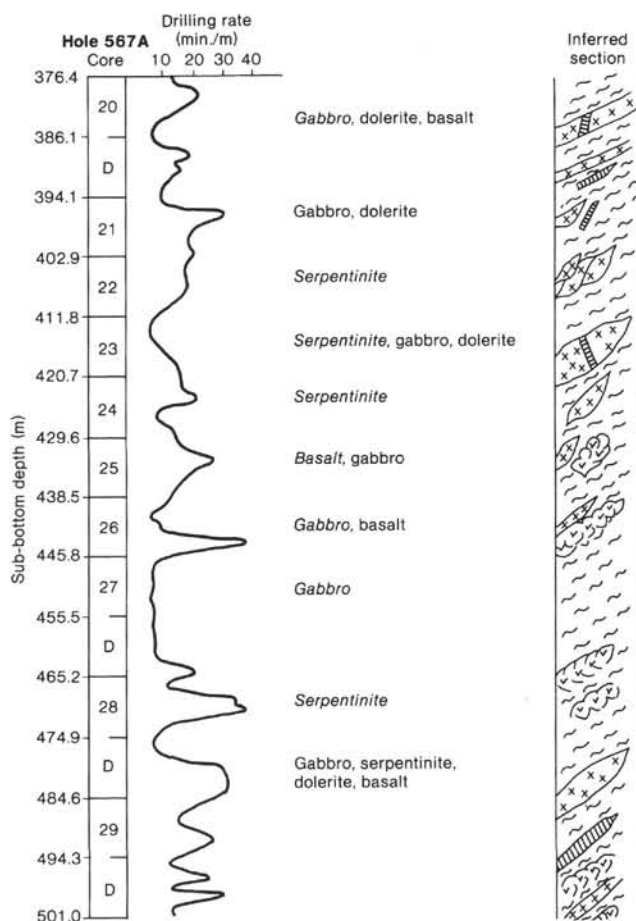


Figure 5. Inferred columnar section at the bottom of Hole 567A, deduced from the drilling rate. Core lithology is listed in the middle column; italicized rock type is predominant. D (drilled) indicates that recovery was combined with recovery of the preceding core, that is, two core lengths were drilled for every instance of recovery.

parts only by chlorite mineralization. Some of the clinopyroxene and olivine grains are weakly kinked.

**Sample 567A-20-1 (Piece 2, 108–111 cm)  
(369.4 m sub-bottom)**

This is an actinolite-rich ultramafic rock. Fibrous aggregate of actinolite is abundant. Grains are mostly contorted or kinked (Fig. 6B). Clinzoisite is seen sporadically. A vein made of tiny prehnite clinzoisite crystals is seen. This is a metasomatic rock commonly observed within serpentinitized ultramafic rocks onland (Nishiyama, 1979).

**Sample 567A-20-1 (Piece 3, 113–116 cm)  
(369.5 m sub-bottom)**

This is a metamorphosed two-pyroxene gabbro. Pyroxene (augite and bronzite) is largely or partly replaced by actinolite both in the rim and core. Plagioclase is partly chloritized. Remarkable kink banding is seen in the pyroxenes. Cataclastic deformation is not seen in the grain boundaries. Analcite and thomsonite are the common zeolite minerals in the vein. Tiny prehnite grains

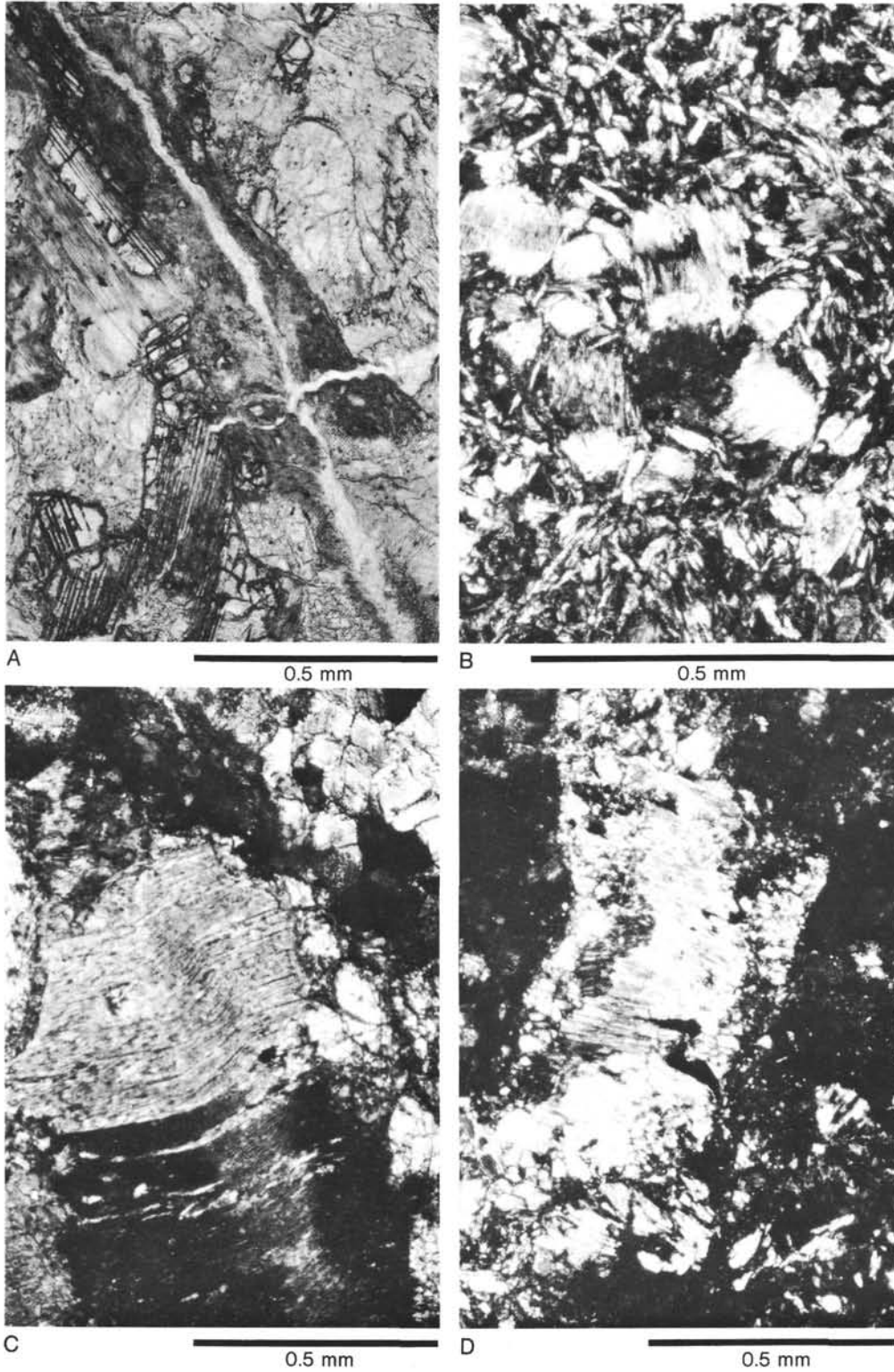


Figure 6. Photomicrographs of ophiolitic rocks from Hole 567A. A. Sample 567A-29-1 (Piece 1, 103–106 cm), showing cataclastic deformation and analcite veins. B. Sample 567A-20-1 (Piece 2, 108–111 cm), showing kinking of actinolite. C. Sample 567A-20-1 (Piece 8, 138–142 cm), showing kinking of tremolite. D. Sample 567A-21,CC (Piece 1, 12–18 cm), showing kinking and cataclastic deformation of hornblende; other areas are occupied by analcite replacing plagioclase. (Fig. 6A is under plain light, others under crossed nicols.)

are observed next to the pyroxenes. The first stage of metamorphism was of greenschist facies, and the last of zeolite facies.

**Sample 567A-20-1 (Piece 5, 125–127 cm)  
(369.7 m sub-bottom)**

This is metabasite, completely composed of intergrowths of chlorite, plagioclase, and sphene. No other minerals remain. This is a greenschist facies metabasite probably derived from doleritic rocks, because ophitic texture remains in some parts. No foliation is seen.

**Sample 567A-20-1 (Piece 8, 138–142 cm)  
(369.8 m sub-bottom)**

This is a coarse-grained two-pyroxene gabbro. Plagioclase is partly saussuritized, and epidote occurs. Remarkable thick veins composed of epidote and calcite occur. Around the vein walls, kinked and folded amphibole (tremolite) is common (Fig. 6C). The tremolite is crushed in a cataclastic fashion. This is metamorphic rock of the lower part of the amphibolite facies. Plagioclase is partly replaced by chlorite. This may be a retrogressive phase.

**Sample 567A-21,CC (Piece 1, 12–18 cm)  
(402.9 m sub-bottom)**

This is a coarse hornblende gabbro. Plagioclase is highly saussuritized, and green hornblende is partly chloritized or actinolitized in the rim. Remarkable fracturing occurs, and some hornblende grains show weak kinking (Fig. 6D). An analcite vein intrudes the deformed texture. The rock was originally a hornblende gabbro, but was then metamorphosed into a greenschist facies, and finally retrogressively altered in the zeolite facies.

**Sample 567A-25-1 (Piece 4, 33–44 cm)  
(429.9 m sub-bottom)**

Piece 4 was observed on board and Piece 6A (described later) was observed onshore, but judging from the similar internal features of the two, they may be from the same rock body, fractured during the drilling. This rock is an alkali pillow basalt, showing gradual change of texture and composition from the core to rim (Figs. 7 and 8). In the inner part, ophitic to intergranular texture predominates, containing mostly plagioclase and titanite. The texture is not as highly altered or deformed but shows contorting in the original plagioclase. Calcite and zeolite veins cut the inner part of the pillow in two directions. Zeolite is analcite, which commonly occurs in alkali rocks. Toward the rim, the texture grows finer-grained as a result of both earlier cooling and later pulverization. In the rim, which occupies about half of the thin section, texture is cataclastic, characterized by a mixture of different kinds of small fragments of basaltic origin and their related materials containing volcanic shale (Figs. 7 and 8). These textures indicate a high degree of shearing under considerably high temperature, which caused ductile deformation (E. Rutter, personal communication, 1983). This zone contains at least the following components: (1) Greenish homogeneous clayey devitrified glass, which occupies a

large proportion of the section, is present. (It is partly phacoidal or lens shaped.) (2) Also present is orange fine-grained pulverized basalt, which is highly crushed along the boundaries between the basalt proper and its covering layer described later. (Fragments of basaltic rocks of variolitic texture, which is different from the ophitic-intergranular texture in the core, are recognized. Fragments of basalt that originally contained phenocrysts or microphenocrysts of augite that are now fully pulverized also occur in this area.) (3) Reddish fine materials of muddy metallic sediments occur, which include many fragments of basaltic and other materials such as foraminifers (planktonic type, probably younger than the Jurassic, D. Carter, personal communication, 1983) and spumellarian-type radiolarians (Fig. 7B and C). (This zone is opaque in plain light.)

These observations indicate that the rim of the basalt is highly pulverized, sheared, and fragmented, making a complicated shear zone of basalt and pelagic sediments that contain microfossils, although the core does not show any significant deformation. The pulverization occurred; then fragmentation and rotation produced by shearing followed. Some fragments of basalt and glass show rotation tails by shearing. Calcite veins in Figure 8 show two shear zones: one shows a right lateral sense of offset in the thin section, the other a left lateral sense. The reddish black metallic materials may be the same as the umberlike sediments deposited just on the basalt surface indicated in Sample 567A-26-1 (Piece 4) and discussed later; these occur in many parts of shear zones (Fig. 9). This indicates an injection of ductile materials during the shearing.

The basalt is similar to or the same as the alkali basalt of Sample 567A-25-1 (Piece 6A), described next and is probably pillow lava. The calcite veins may fill early-formed cracks in the pillow. Some fragments on the sheared part may be broken from the pillow or may be hyaloclastic materials.

**Sample 567A-25-1, (Piece 6A, 54–60 cm)  
(430.1 m sub-bottom)**

Some parts of the section were analyzed by Electron Microprobe (Tables 1, 2, and 3). About half of the section is occupied by brownish amorphous to devitrified glass, which shows typical spherulitic texture (Fig. 8). This is at least 1 cm thick in the thin section and is in contact with basalt of intersertal texture. Zeolite minerals (analcite, phillipsite, and stilbite) fill in the piece, which also includes clay minerals. This part was originally the outer glassy crust of the pillow. The inner part is composed of basalt of intersertal texture and contains black metallic materials of irregular shape. Many spots of greenish clay are included within this metallic halo. Electron Microprobe analysis (Table 2) indicates that the metallic material is an Fe-rich hydrosilicate and hydroxide mixture like Cyprus umber (Robertson and Hudson, 1973). The total iron oxide (FeO\*) content of the Cyprus umber and of the metallic sediment of this study do not differ greatly, but MnO<sub>2</sub> content in the latter is lower. The greenish clay minerals are K-rich celadonite and glauconite (Buckley et al., 1978) (Table 1) and also re-

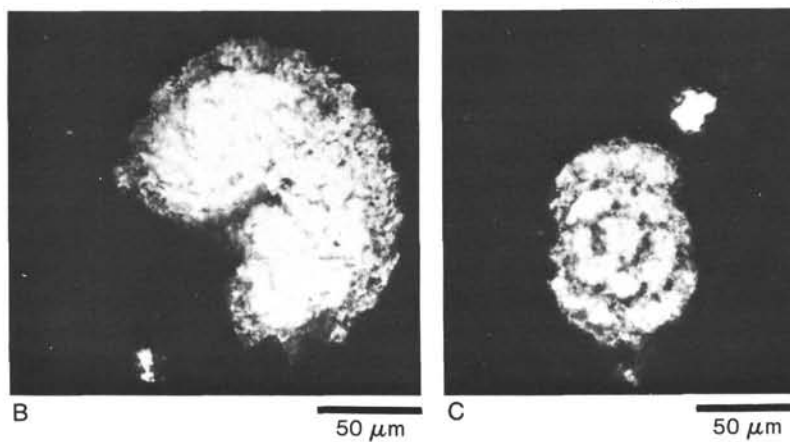


Figure 7. A. Photograph of thin section of basalt, Sample 567A-25-1 (Piece 4, 33-44 cm), showing the rim of alkali pillow basalt. B. and C. Photomicrographs of foraminifers and radiolarians, respectively. Locations shown by arrows in Fig. 7A.

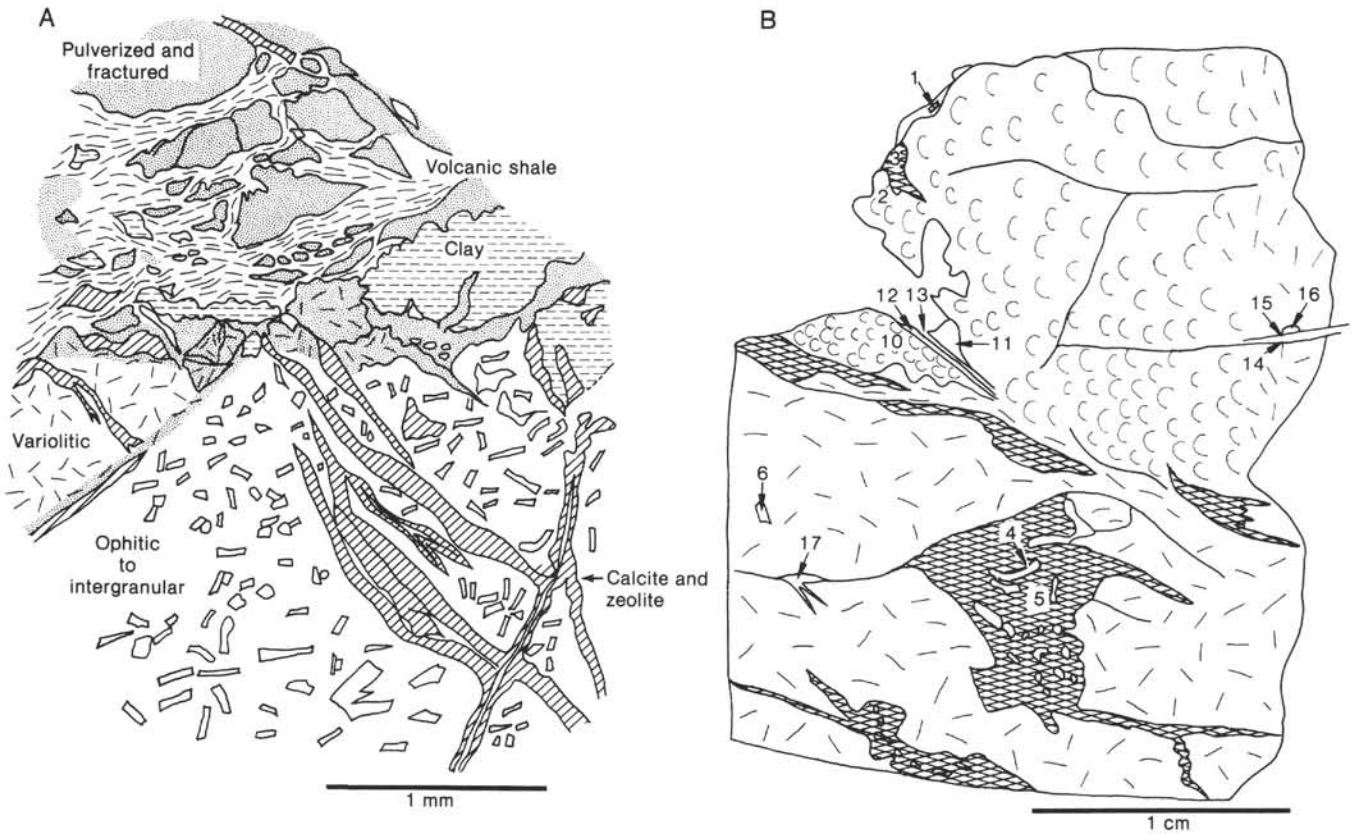


Figure 8. Sketches of thin section of basalt. A. Sample 567A-25-1 (Piece 4, 33-44 cm), showing pulverization and fracturing on the rim of pillow basalt. B. Sample 567A-25-1 (Piece 6A, 54-60 cm); numbers show microprobe analysis (see Tables 1 to 4).

place the groundmass of the basalt itself. Such an enrichment of  $K_2O$  in the basalt is known from the weathered basalt in the Pacific and Atlantic seafloor (Humphries et al., 1980; Morrison and Thompson, 1983), but comparison of the clays in this study with those in the Pacific and Atlantic shows that these have a very high  $K_2O$  content and low  $MgO$  content, whereas  $FeO^*$  is similar. The zeolites mentioned earlier occur in the vein as the last products of alteration (Table 3).

**Sample 567A-25-1, (Piece 5, 47-51 cm)  
(430.1 m sub-bottom)**

This is a highly sheared metabasite or metadolerite. This section shows an intergranular texture of plagioclase laths, titanite and many veins of opaque minerals. Shearing is extremely strong and many shear planes intersect each other. Plagioclase laths are curved and rotated. This deformation may have occurred under high temperature for ductile conditions. Calcite, zeolite, and clay and opaque minerals are seen in many small veins. Blocks of intersertal basalt are enclosed within the shear zone.

**Sample 567A-25-1 (Piece 15, 127-131 cm)  
(430.9 m sub-bottom)**

This is an alkali basalt that is intensely sheared (Fig. 10A). The main part is the core of basalt, probably of pillow basalt, with an intersertal texture, now largely pulverized; it is intruded by many veins of opaque minerals. Several shear zones made of blocks of basalt and

clay minerals occur. Spherulitic clays are brownish, partly similar to the devitrified glass such as in Sample 567A-25-1 (Piece 6A). Grains in the shear zone are highly pulverized and rotated by zone shearing. Chlorite is interpreted to be an alteration mineral, because it is developed within a rounded devitrified fragment. Analcite veins cut all other textural features, suggesting they formed late.

**Sample 567A-26-1 (Piece 1, 0-8 cm)  
(438.5 m sub-bottom)**

This is a rim of an alkali pillow basalt (Figs. 10 and 11). A notable shear zone occurs between the core and rim. The rim is composed of many different kinds of rock fragments in a sheared matrix of pulverized fine basaltic fragments, reddish volcanic shale, and metallic sediment. Such a feature is similar to Sample 567A-25-1 (Piece 4). The core is of hyalophitic to intersertal texture, consisting of titanite phenocrysts and plagioclase laths. The augite contains 2.41 to 2.67%  $TiO_2$  (Table 4). Very fine material lies within a 10-mm width along the outer side of the core. The zone contains rounded, phacoidal, or angular fragments of the following materials (Fig. 11): (1) basalt of hyalophitic to intersertal texture that has no green clay minerals (this feature is the same as much of the inner part of the section); (2) basalt of intersertal texture but that has a green clay mineral (this clay is identified as celadonite or glauconite by electron microprobe analysis [Table 1]); (3) basalt of trachytic texture (plagioclase laths are

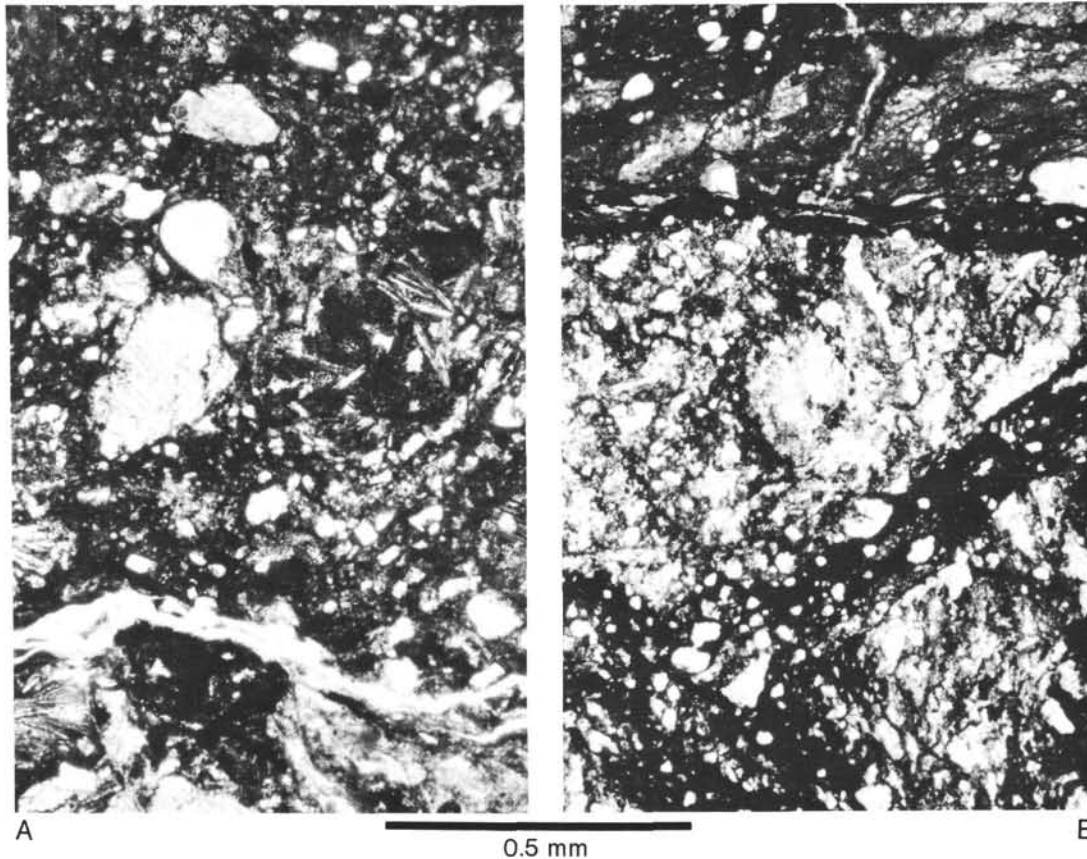


Figure 9. Photomicrographs showing cataclastic deformation and fracturing in basalt rim, Sample 567A-25-1 (Piece 4, 33–44 cm). A. Note that the intergranular texture remains in the fragment, and an analcite vein cuts the cataclastic texture. B. The intergranular texture in the fragment is fully cataclastically deformed and pulverized grains (white) float in the metallic vein (black) injecting the rim.

aligned in parallel; these grains occur close to the outer part of the zone).

All these grains are rounded, phacoidal, or lenticular, and the matrix of the grains is composed of pulverized local basalt, reddish volcanic shale, or metallic sediments (Fig. 11). Almost opaque metallic sediments, similar to the umberlike sediments mentioned earlier, also occur.

**Sample 567A-26-1 (Piece 15, 107–113 cm)  
(439.6 m sub-bottom)**

This is an alkali dolerite of ophitic to subophitic textures. Large titanite crystals are common. Glass is altered to montmorillonite or chlorite. Heulandite and prehnite veins are present, and no strong deformation is observed.

**Sample 567A-28-1 (Piece 1, 44–53 cm)  
(455.9 m sub-bottom)**

This is a serpentinite altered from harzburgite. Serpentine is largely made of lizardite and chrysotile now of a mesh texture and of poor crystallinity. The grains are usually kinked. Grains are large—about 1 to 2 mm in diameter—and show original layering, suggesting the cumulate origin.

Other serpentinite sections were also examined, but most were similar to those described. The volumetric ex-

tent shows olivine from 71 to 86%, and orthopyroxene from 29 to 14%. Chrome spinel ranges from 1 to 4%.

**Site 569**

This site is located on the lower part of the middle Trench slope, 32 km landward from the Trench axis at a depth of 2770 m. Below a thick 351.4 m sedimentary cover as old as late Eocene, 9.5 m of altered amphibolite were drilled at Hole 569A. No other kinds of basement rocks were recovered. The nature of the contact between the basement and the Eocene sedimentary rocks is not well known. Early to late Eocene sedimentary rocks are not like others recovered on the Guatemalan slope (Aubouin, von Huene, Azéma, et al., 1982). They are dark green to black siliceous radiolarian-rich mudstone (see lithology section, Site 569 report, this volume). Radiolarians are stained by metallic minerals (probably iron sulfide), and such features are similar to those at Site 494 of Leg 67 (Aubouin, von Huene, Azéma, et al., 1982). Therefore it is suspected that the 38.3-m-thick Eocene sediments were deposited under rather stagnant conditions around the oxygen minimum zone, probably deposited unconformably upon the ophiolitic rocks in the Trench landward slope.

The altered amphibolite was originally a medium-sized metamorphosed mafic rock, that is a metabasite. The plagioclase between the green hornblende has entirely been

Table 1. Microprobe analysis of clay minerals from basalt (wt. %).

Oxide	Analysis number										
	2	1	11	10	15	16	6	4	9	20	21
SiO <sub>2</sub>	34.00	48.72	46.08	47.43	56.89	54.42	49.50	46.69	51.22	53.85	51.65
TiO <sub>2</sub>	4.97	2.60	4.66	2.07	1.32	0.71	0.07	—	0.17	0.06	0.32
Al <sub>2</sub> O <sub>3</sub>	8.46	12.89	12.97	12.66	16.93	20.90	8.61	6.69	9.50	6.24	13.49
FeO*	15.81	13.73	14.53	9.16	7.14	4.53	19.30	23.35	17.18	18.98	13.96
MnO	0.10	0.10	0.22	0.08	0.22	—	0.05	0.13	0.07	0.04	0.05
MgO	2.54	3.70	4.80	3.05	2.25	1.50	3.80	3.43	3.77	5.07	5.97
CaO	2.90	0.66	0.74	2.19	3.27	7.04	0.63	0.81	0.40	0.25	0.60
Na <sub>2</sub> O	2.68	—	0.36	3.85	6.13	5.15	—	—	—	0.12	0.01
K <sub>2</sub> O	2.21	8.25	7.60	3.88	2.93	2.44	9.22	8.67	9.59	9.96	8.65
Total	73.67	90.65	91.96	84.37	97.08	96.69	91.18	89.77	91.90	94.59	94.70
Element (No. of molecules at O = 22)											
Si		7.27	6.87	7.38	7.50	7.17	7.62	7.52	7.71	7.95	7.35
Al		0.73	1.13	0.62	0.50	0.83	0.38	0.47	0.29	0.05	0.65
Al		1.11	1.14	1.71	2.13	2.41	1.18	0.79	0.55	1.03	1.62
Fe		1.71	1.81	1.19	0.78	0.49	2.48	3.14	2.16	2.34	1.66
Mg		0.82	1.06	0.70	0.44	0.29	0.87	0.82	0.84	1.11	1.26
Ti		0.29	0.52	0.24	0.13	0.07	0.00	0.00	0.01	0.00	0.03
Ca		0.10	0.12	0.36	0.46	0.99	0.10	0.14	0.06	0.04	0.09
Na		0.00	0.10	1.16	1.56	1.31	0.00	0.00	0.00	0.03	0.00
K		1.57	1.44	0.77	0.49	0.41	1.81	1.78	1.84	1.87	1.57

Note: Analysis numbers 2, 1, 11, 10, 15, 16, 6, and 4 are from Sample 567A-25-1 (Piece 6A, 45–60 cm), and analysis numbers 9, 20, and 21 are from Sample 567A-26-1 (Piece 1, 0–8 cm). See Figures 8 and 11. A brief explanation of each spot analysis number follows: 2—brownish spherical aggregate of weakly crystallized glass in the outermost rim; 1—pale green to yellow grain in zeolite vein; 11—pale green to yellow grain in zeolite vein; 10—brownish spherical aggregate near basalt core; 15—yellowish green grain in the wall of zeolite vein; 16—pale green grain in the matrix of spherical aggregate; 6—pale green matrix in the intersertal texture; 4—fresh green grain in calcite vein; 9—fresh green grain in calcite vein; 20—fresh green (low birefringence) grain in volcanic shale; 21—pale green (high birefringence) grain in volcanic shale. — means no detection or trace. Blank in the Analysis number 2 column means no calculation.

Table 2. Microprobe analysis of metallic sediments (wt. %).

Oxide	Analysis number	
	3	5
SiO <sub>2</sub>	22.17	20.16
TiO <sub>2</sub>	4.12	8.28
Al <sub>2</sub> O <sub>3</sub>	5.33	4.93
FeO*	52.38	49.52
MnO	0.25	0.32
MgO	3.18	2.25
CaO	0.73	1.78
Na <sub>2</sub> O	0.07	—
K <sub>2</sub> O	3.24	2.90
CrO	0.17	—
NiO	—	1.13
Cl	0.05	0.04
Total	91.68	90.29

Note: Analysis numbers from thin section of Sample 567A-25-1 (Piece 6A, 45–60 cm). See Figures 8 and 11. — means trace or not detected.

altered to zeolite and prehnite (Figs. 12 and 13). Hornblende is also locally changed along the crystal edge to chlorite. The zeolite mineral is natrolite. Some sections show a weak foliation (Fig. 12B). Other deformation is not well known, but the following history can generally

Table 3. Microprobe analysis of zeolite minerals (wt. %).

Oxide	Analysis number					
	12	13	14	17	18	19
SiO <sub>2</sub>	56.09	55.54	55.56	58.55	54.29	54.47
TiO <sub>2</sub>	0.12	0.12	0.09	0.68	0.03	—
Al <sub>2</sub> O <sub>3</sub>	21.13	22.12	22.12	17.41	20.72	20.69
FeO*	0.05	0.12	0.31	0.24	0.07	0.15
MnO	—	0.02	—	—	0.04	—
MgO	0.03	—	0.20	—	0.02	—
CaO	0.04	2.24	0.09	5.13	0.09	0.14
Na <sub>2</sub> O	12.56	5.49	13.77	1.86	12.66	12.59
K <sub>2</sub> O	—	7.87	0.04	2.35	—	0.02
CrO	0.51	—	—	0.01	0.01	—
NiO	0.16	0.05	—	—	—	0.06
Total	90.23	93.58	92.18	86.22	87.92	88.13
Name of mineral	Analcite	Phillipsite	Analcite	Stilbite	Analcite	Analcite

Note: Analysis numbers 12, 13, 14, and 17 are from Sample 567A-25-1 (Piece 6A, 45–60 cm). Analysis numbers 18 and 19 are from Sample 567A-26-1 (Piece 1, 0–8 cm). — indicates trace or not detected.

be recognized. First some mafic rock, probably gabbro or dolerite, was metamorphosed into a hornblende schist of amphibolite facies, and then it was further altered to zeolite facies hydrothermally. Hydrofracturing may have occurred in this stage, because most of the sections show remarkable veining along irregular planes containing various brecciations. A brief description of each section follows.

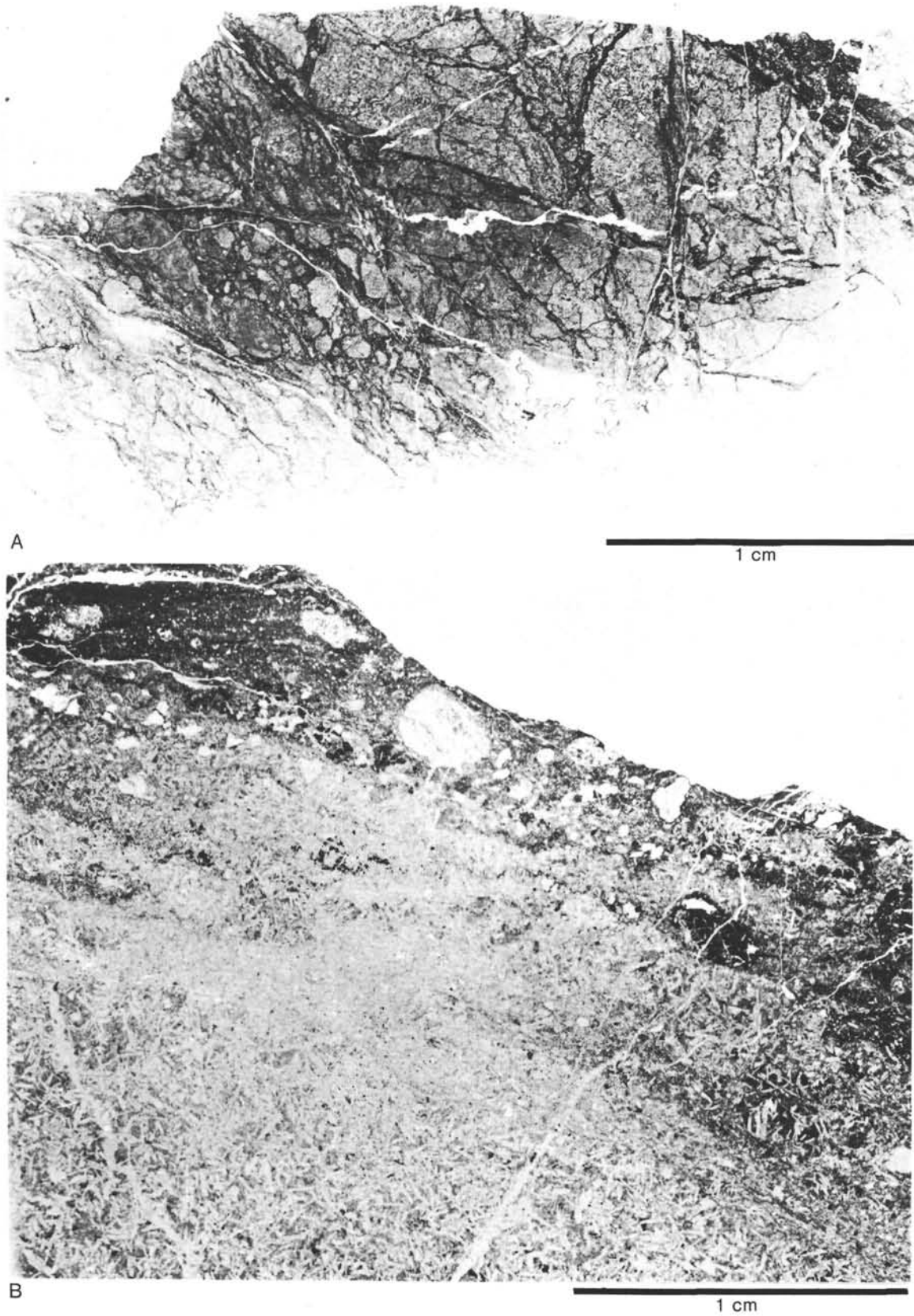


Figure 10. Photographs of thin sections of basalt. A. Sample 567A-25-1, (Piece 15, 127–131 cm) shows abundant shearing and pulverization. B. Sample 567A-26-1 (Piece 1, 0–8 cm) shows cataclastic deformation and shearing on the rim of pillow basalt. See also Figure 11.

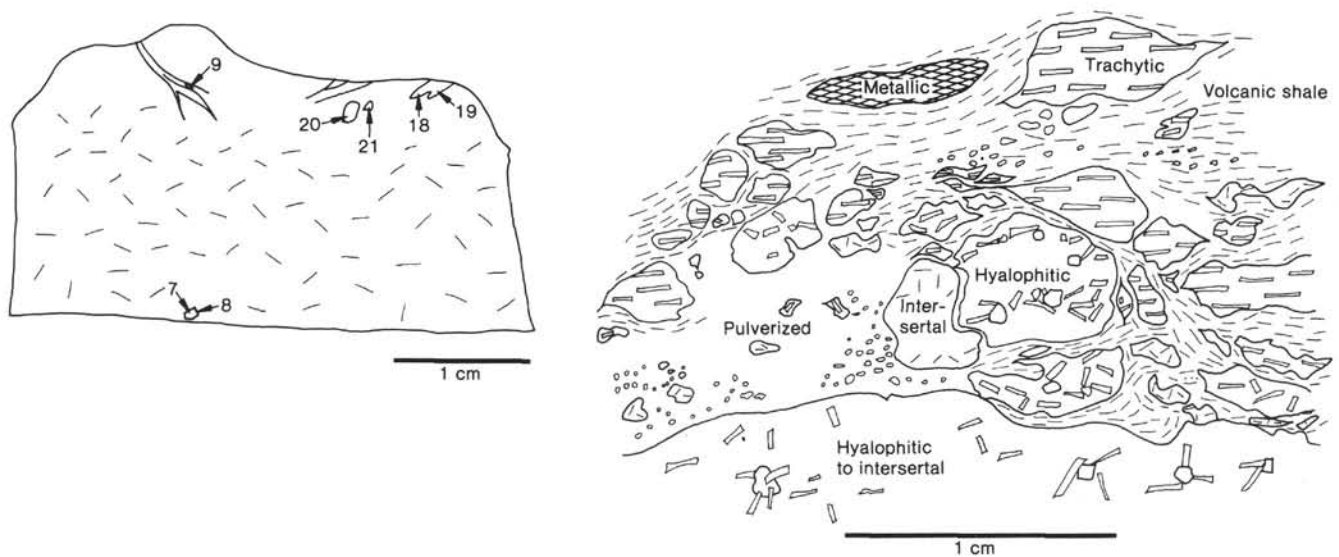


Figure 11. Sketch of thin section under microscope of the same area as Figure 10B, Sample 567A-26-1 (Piece 1, 0–8 cm). Note that pulverization and shearing are notable over different fragments of texture. On the left, the microprobe analysis locations are shown (see Tables 1 to 4).

Table 4. Microprobe analysis of titanite from basalt (wt. %).

	Analysis number	
	7	8
Oxide		
SiO <sub>2</sub>	47.60	47.23
TiO <sub>2</sub>	2.41	2.67
Al <sub>2</sub> O <sub>3</sub>	3.72	3.77
FeO*	12.58	12.01
MnO	0.46	0.35
MgO	10.47	11.11
CaO	20.71	20.44
Na <sub>2</sub> O	—	—
K <sub>2</sub> O	0.12	—
CrO	0.12	0.08
NiO	0.08	0.14
Cl	0.06	0.03
Total	98.20	97.82
Element		
O	6.000	6.000
Si	1.773	1.745
Al	0.163	0.164
Mg	0.582	0.612
Ca	0.827	0.809
Ti	0.067	0.074
Fe	0.392	0.371
Mn	0.014	0.011

Note: Analysis numbers are from Sample 567A-26-1 (Piece 1, 0–8 cm). — means trace or not detected.

#### Sample 569A-10-1 (Piece 3C, 49–57 cm) (351.9 m sub-bottom)

In this section a few plagioclase grains remain, but most are replaced by natrolite and prehnite. A small amount of quartz is also present.

#### Sample 569A-10-1 (Piece 5, 93–102 cm) (352.3 m sub-bottom)

The plane of the thin section shows apparent thrust faults with several millimeters dislocation. Kinking of prehnite is observed. Hornblende is commonly fractured by the veins made of prehnite and natrolite. At some places natrolite veins cut the prehnite veins. Small amounts of quartz and plagioclase are also present.

#### Sample 569A-10-1 (Piece 9, 128–133 cm) (352.7 m sub-bottom)

A prehnite vein cuts the hornblende, and this vein is further cut by the natrolite vein (Fig. 13B).

#### Sample 569A-10-2 (Piece 1, 33–45 cm) (353.2 m sub-bottom)

Veins made of prehnite and natrolite largely dissect the whole of the section. A prehnite vein is cut by another prehnite vein. Hornblende crystals are about 0.1 to 0.2 mm in diameter, and are roughly arranged in a weak foliated fashion (Fig. 12B). A large amount of chlorite occurs as veins and fibrous aggregates. Quartz is also present.

#### Site 570

This Site is located at the lower edge of the upper Trench slope, 42 km landward from the Trench axis at a depth of 1698 m. Below a sub-bottom depth of 374.0 m, penetration of a sedimentary cover as old as early Eocene, was accomplished, and 27.9 m of serpentinite were drilled. The 44-m-thick Eocene section is quite different from the Eocene section of Site 569 discussed earlier. It is composed of alternating layers of siliceous limestone and coarse sandstone or conglomerate that includes acid volcanic serpentinite, although no fragments of serpentinite were contained in the overlying strata.

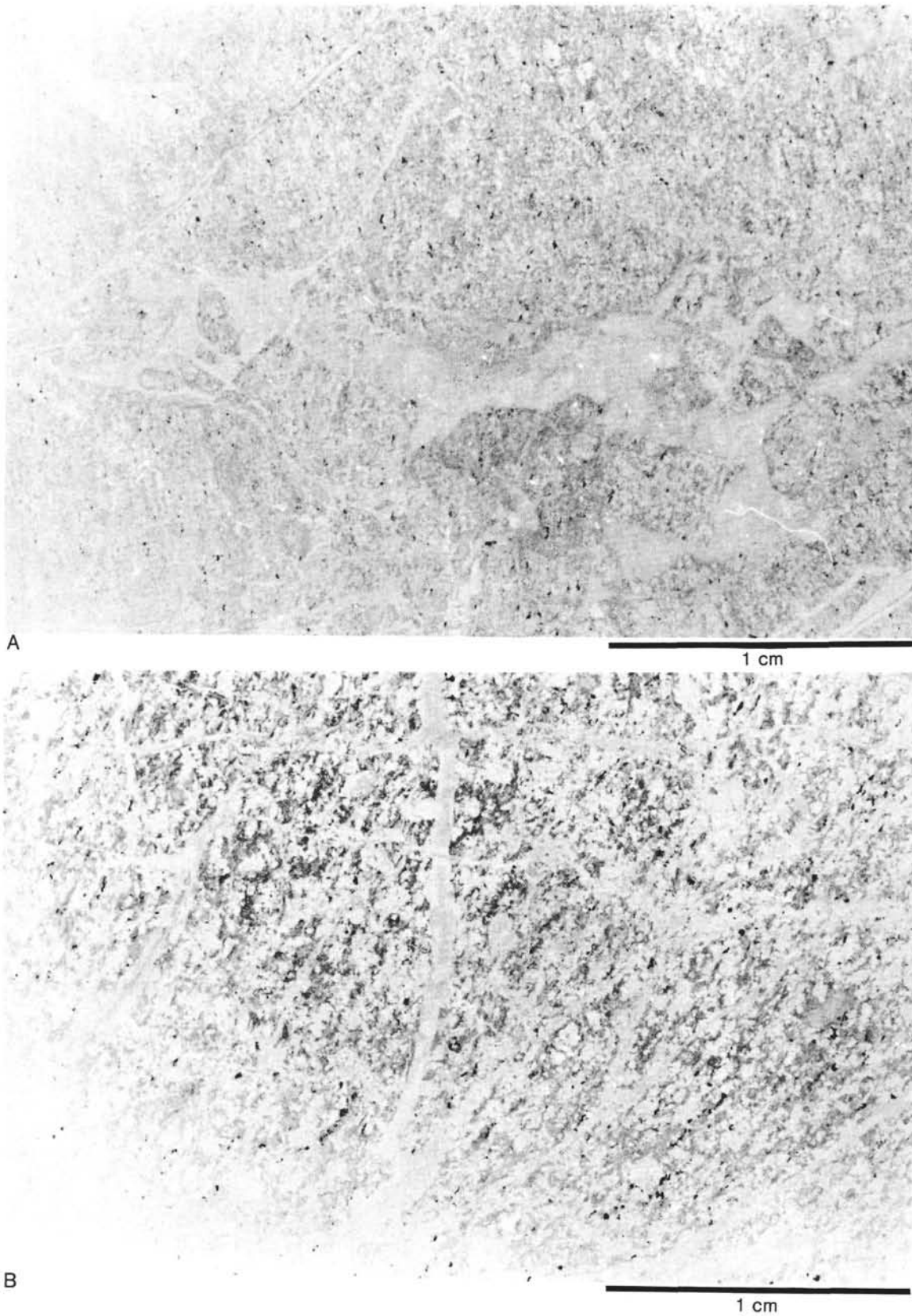


Figure 12. Photomicrographs of thin sections of altered amphibolite. A. Sample 569A-10-1 (Piece 5, 93–103 cm), showing irregular thick veining made of prehnite, like hydrofracturing. B. Sample 569A-10-2 (Piece 1, 3–30 cm), showing gentle foliation and abundant veining of prehnite. In both sections, plagioclase is totally replaced by natrolite. See Figure 13 also.

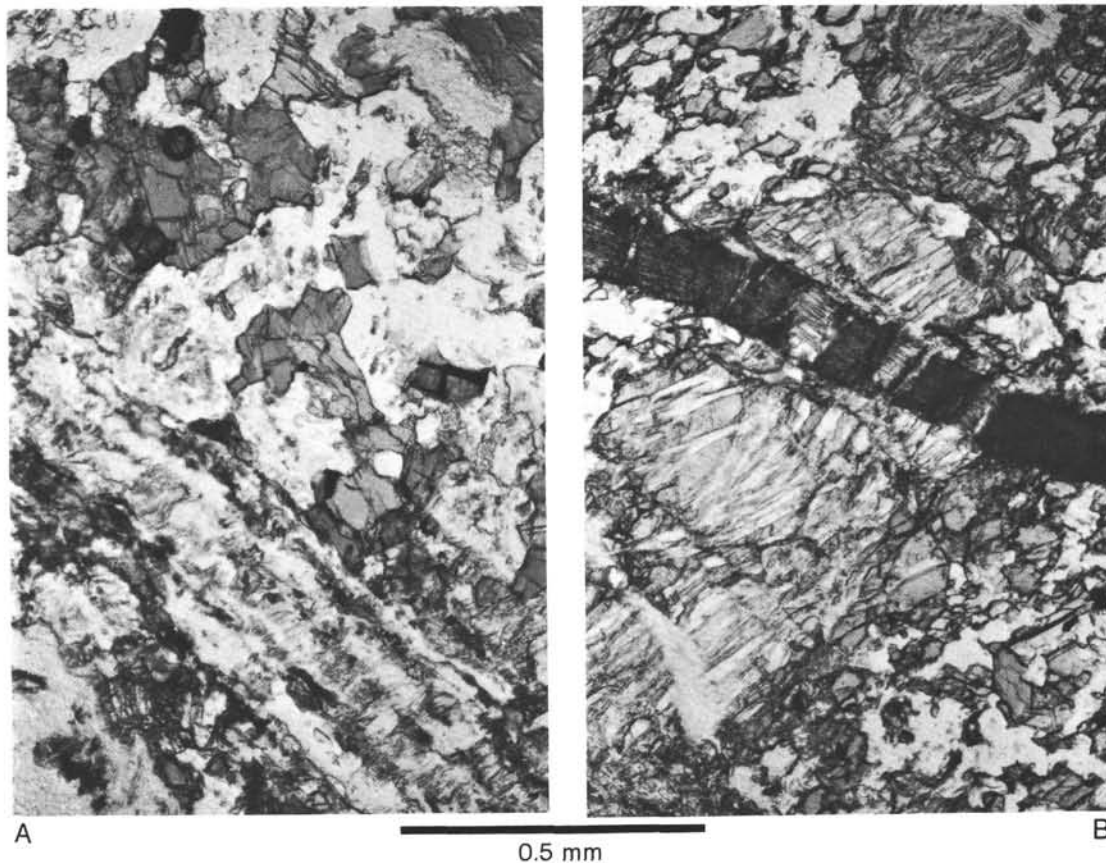


Figure 13. Photomicrographs of altered amphibolite. A. Sample 569A-10-1 (Piece 3C, 49–57 cm), showing prehnite vein cutting amphibolite already altered by natrolite. B. Sample 569A-10-1 (Piece 9, 128–133 cm), showing a thick prehnite vein cut by a natrolite vein.

Two thin sections of serpentinite (Samples 570-41-3, Piece 7, 385.4 m sub-bottom and 570-42-2, Piece 5, 394.5 m sub-bottom) were examined. Serpentinite is largely serpentized harzburgite, the original composition of which contained 74 to 79% olivine and 26 to 21% orthopyroxene, with a trace of chrome spinel. The crystals are coarse and roughly foliated, probably cumulate peridotite or tectonized harzburgite.

#### DISCUSSION: EMPLACEMENT OF THE OPHIOLITIC ROCKS IN THE FOREARC AREA

The rocks described in this chapter are composed of many varieties of ultramafic to mafic igneous rocks. In addition to typical ophiolitic rocks, Leg 84 recovered igneous rocks of alkali as possibly island-arc affinities, as discussed later. The whole assemblage of these rocks, however, is considered an ophiolitic *mélange*, characterized by a disturbance of metamorphosed and sheared mafic rocks within highly serpentized peridotite in a dismembered fashion. The primary metamorphic grade ranges from amphibolite to greenschist facies and is further overprinted by much lower grades of zeolite facies, sometimes characterized by a prehnite–actinolite assemblage. These rocks are generally altered and veined. Most of the rocks show some shearing and cataclastic deformation. Folding also occurs and may have developed under relatively ductile conditions, because it is associated with flow by pulverization.

Cataclasis is common in gabbros and pillow basalts. The cataclasis may have taken place after calcite veining and clay mineral alteration, probably occurring on the seafloor, but definitely before zeolite veining. Pillow basalt also shows intense shearing along the rim, including mixing with pelagic sediments. The mixed pelagic sediments include amber or volcanic shale, which contains celadonite, glauconite, and other altered minerals as well as microfossils. Cataclasis in the basaltic texture was followed by large-scale fragmentation of the rocks. Folding in the gabbroic rocks occurred after greenschist facies metamorphism and was followed by cataclastic deformation along fault planes, in turn followed by zeolite veining. The deformation sequence and mineralization described earlier occur in almost all rock types and are characteristic of phenomena occurring at relatively high temperature, as mentioned before. It is known from triaxial experiments that cataclasis of basaltic rocks is a typical deformational feature under considerably high temperature and hydrated conditions—it is the initiation of fracturing (Rutter et al., 1982).

As briefly mentioned, some rocks may be part of a typical ophiolitic assemblage, but others may be of different origin. Harzburgite and lherzolite are commonly in the lowest levels of the ophiolitic sequence, composing layer 4 in the oceanic crust as well as the upper mantle (Gass and Smewing, 1981). The banded or foliated texture indicates ultramafic cumulate origin. Possibly

most of the drilled serpentinites were highly sheared originally, but this texture was probably destroyed during drilling. Extremely abundant harzburgite may indicate the different origin of the ultramafic part of the drilled ophiolitic rocks. Harzburgite is not very common in the spreading ridge or ridge-ridge transform faults, but is quite common in the orogenic (or Alpine type) ophiolite and has recently been found in several forearc ophiolite occurrences along the Izu-Bonin-Mariana arc (Bloomer 1983; Bloomer and Hawkins, 1983). This fact may suggest other possibilities for the emplacement of ophiolitic rocks in the island-arc area as well as in the orogenic area, as discussed later.

Three kinds of gabbros occur: an olivine-clinopyroxene gabbro, a two-pyroxene gabbro, and a hornblende gabbro. The first and the last of these are quite common in ophiolitic rocks, but the two-pyroxene gabbro is not common in the ophiolite found in the spreading ridge areas such as along the Mid-Atlantic Ridge. It may be related to some island-arc-type magmatism incorporated into the ophiolite *mélange* mass. Actinolite rock is very common as a nodule of ultramafic rock in a serpentinite belt, occurring as a result of metasomatism between peridotite and basalt (Nishiyama, 1979). Some dolerite and all basalts observed in this study are characterized by titanite. These rocks are probably all alkaline rocks, commonly associated with volcanic islands seamounts. We found no tholeiitic rocks that are typical of ophiolitic assemblages, but samples collected by Tournon et al. (this volume) include some tholeiitic basalt, judging from the chemical analysis. Such a variety may be caused by the poor recovery and sparse sampling.

Chemistry and petrology of all mafic and ultramafic rocks must be further studied in detail but the rocks can be principally characterized as of oceanic origin, with some island arc rocks. Few pelagic sedimentary rocks occur, except for the thin cover on the alkali pillow basalt and the Late Cretaceous limestone above the ophiolitic rocks. The latter was either originally deposited upon the oceanic plate or volcanic island or was later emplaced during tectonism or slumped from upslope.

Magnetic and gravitational anomalies that could characterize mafic or ultramafic rocks at shallow depth extend from the area off the Guatemala Trench slope as far south as the Nicoya Peninsula of Costa Rica (Von Huene, Aubouin, et al., 1980). On the Nicoya Peninsula a Jurassic to Cretaceous basalt-chert sequence outcrops extensively with Tertiary island-arc sedimentary rocks (Schmidt-Effing, 1979; Galli-Olivier, 1979; Kuijpers, 1980; Lundberg and Moore, 1982; Gursky et al., 1982; Azéma and Tournon, 1982). The Nicoya sequence is interpreted either as an oceanic plate fragment accreted to the Caribbean Plate or as a mixture of an aseismic ridge and island-arc bodies. In either case, the ophiolitic rocks underneath the Trench landward slope off Guatemala appear to continue to the Nicoya Peninsula or around the Trench slope or slope break direction.

At four Leg 84 Sites (Sites 566, 567, 569, and 570), which range over about 50 km perpendicular to the Trench axis, ophiolitic rocks were recovered. We believe that the entire slope landward of the Trench is underlain

by the tectonized ophiolitic material (Aubouin, von Huene, Baltuck, et al., 1982). Some of the parts of the ophiolitic rocks may extend landward to the basaltic layer that is supposed to be underneath the thick sedimentary pile of the forearc basin (Seely, 1979).

The emplacement of the basaltic rocks in the Nicoya Peninsula is considered to have taken place in two stages—in the Late Cretaceous and middle Tertiary (Kuijpers, 1980). The structure and deformation indicate that the rocks suffered strong lateral shortening by folding and thrusting, but seem not to show any subduction-related metamorphism and deformation in the later Cretaceous. In the Tertiary sections there is abundant evidence of arc volcanism, suggesting the active subduction of the Cocos Plate (Kuijpers, 1980; Gursky et al., 1982). In Guatemala, thick Cretaceous to Recent forearc basin sediments have accumulated (Seely, 1979). The origin of the forearc basin extends back to the same stage of the Cretaceous (Lundberg and Moore, 1982). There are still not enough data to relate the dredged ophiolitic rocks to those onland; the emplacement of the ophiolitic rocks to those onland; the emplacement of the ophiolitic rocks occurred before early Eocene, as already indicated, but possibly earlier during the Cretaceous when the arc-trench system of this region began to form (Lundberg and Moore, 1982).

Other examples of forearc ophiolite have been recently reported in the western Pacific regions (Crawford et al., 1981; Dietrich et al., 1978; Bloomer and Hawkins, 1983; Ishii, 1983; Hussong and Fryer, 1983; Ogawa and Naka, 1984; Ogawa, 1983). These areas have dismembered ophiolitic rocks from the foot of the Trench landward slope to the upper slope areas (Fig. 14). The general occurrence, assemblages, and characteristics are all very similar to each other in degree of metamorphism and style of deformation. All of the examples contain rocks indicating cataclastic deformation and metamorphism from amphibolite to greenschist facies with alteration by prehnite-actinolite or zeolite. Furthermore, these examples are also very similar to those of the ophiolitic rocks from the transform faults or fracture zones of the Pacific and Atlantic oceans (Fox et al., 1976; Bonatti, 1976; Bonatti and Hamlyn, 1981).

In these cases an important consideration is to distinguish the tectonic context for the original emplacement of such ophiolitic rocks. Usually ophiolite is considered to originate as oceanic crust and upper mantle produced in the spreading ridge (Bonatti and Hamlyn, 1981; Gass and Smewing, 1981). The basalts are usually tholeiitic (mid-ocean ridge basalt, or MORB), although some so-called "ophiolite" onland may include volcanic island-arc materials, such as the example in the Troodos ophiolite of Cyprus (Myashiro, 1973). Recent results of chemical analysis of some of the forearc ophiolites mentioned earlier indicate that most of the basaltic rocks are not of MORB type but of arc basalt including some volcanic island (seamount) types (Bloomer and Hawkins, 1983; Bloomer, 1983; Ishii, 1983). In some cases boninite (high magnesium, high silica rock) is included. The tectonic significance of the Guatemalan ophiolitic rocks mentioned here is not clearly identified but the general

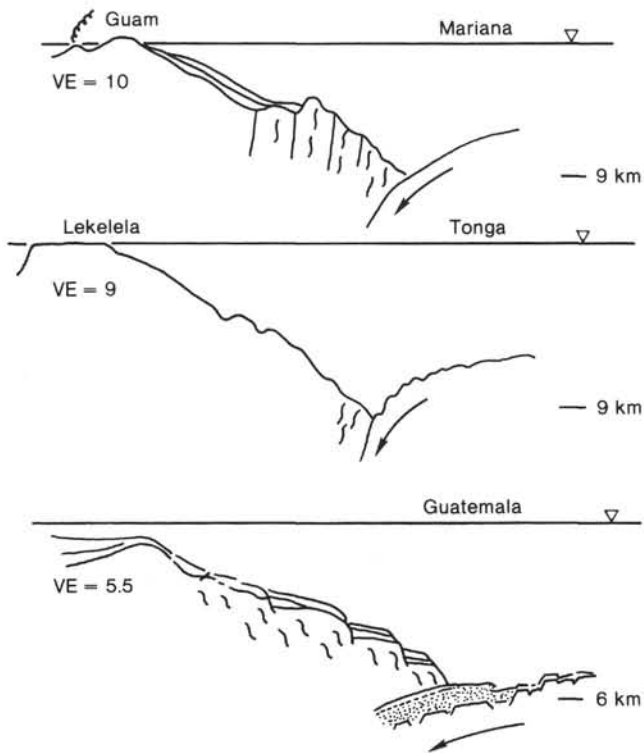


Figure 14. Schematic cross sections of forearc ophiolite-bearing arc-trench systems, including the Middle America Trench off Guatemala. (VE = vertical exaggeration).

assemblages of minerals and rock types suggest several possibilities. Alkalic rocks are common in oceanic volcanic islands and seamounts, and two-pyroxene gabbro is common in island arcs. Furthermore, harzburgite is the most common ultramafic rock constituent in juvenile arcs, such as occurs in the depleted material of boninite (Kushiro, 1983).

The poor recovery and sparse sampling of the drilled materials discussed prevent a study in greater detail, but results of this work show that there are several rock types mixed together within the ophiolitic mélange. The mechanism that produced the Trench landward slope area is not yet known, but three possibilities are suggested:

1. The entire ophiolite was originally a single body produced along the spreading ridge, largely serpentized at the time of spreading (Francis, 1981), and deformed and metamorphosed under the strong shearing and high-grade geothermal conditions present at that time possibly including ridge-ridge transform faults (Fox et al., 1976; Karson and Dewey, 1978) (Fig. 15). Such a scenario for the origin of an ophiolite mélange is discussed by Karson and Dewey (1978) and Casey et al., (1981) for the Bay of Islands ophiolite in Newfoundland and by Ogawa (1983) and Ogawa and Naka (1984) for the Mineoka and Setogawa forearc ophiolites in central Japan. In these cases the alkali basalts are considered to have been produced along the fracture zones. This idea is useful in explaining the cataclastic deformations, mineral veining, and metamorphism, observed off Guatemala, but cannot explain the arc-type igneous rocks

that are sometimes included within or occupy a considerable part of the ophiolitic mass.

2. The entire ophiolite is emplaced just under the arc as materials produced at the beginning of the development of arc magmatism. Such a possibility is suggested by Dietrich et al. (1981), Crawford et al., (1981), Bloomer and Hawkins (1983), Bloomer (1983), and Ishii (1983) for the dismembered ophiolites dredged along the Trench landward slope areas in the Bonin, Mariana, and Yap island arcs (Fig. 16). This idea is based on chemical analysis using trace elements and rare earth elements. In this case the alkali basalt is considered to be seamount material trapped by obduction when ocean floor material was first emplaced at an initial stage of subduction (Bloomer, 1983; see Fig. 16). They consider most of the ophiolitic rocks in the Trench slope area to have originated during arc magmatism. This discussion favors the origin of basaltic and ultramafic rocks, but can explain neither the scarcity of andesite and other felsic igneous rocks that should be associated with arc magmatism nor the origin of some thick pelagic sediments accumulated on ophiolitic rocks. Accumulation of such sediments requires a long time of deep sedimentary environment far from the land derived sediment. Metamorphism and deformation under the forearc area are not well characterized, so we are unable to address how well this model explains the high geothermal conditions and strong shearing of materials observed off Guatemala.

3. The ophiolite mélange is a mixture of several different magmatic types, including mid-oceanic ridge, seamount, and island arc; the mélange was formed along a large fault or fracture zone. This hypothesis covers many possible cases concerning chemical, deformational, and metamorphic history, but includes many uncertainties that cannot be resolved without further chemical, mineralogic, and deformational studies of ophiolite mélange in general and of the ophiolitic rocks drilled off Guatemala in particular.

## SUMMARY

The description and discussion of some ophiolitic rocks drilled at the Trench landward slope area off Guatemala reveal that there is a wide variety of types of magmatism, metamorphism, alteration, and deformation represented. The types of rocks range from basaltic rocks, including alkali basalt, alkali dolerite, gabbro, and metabasite (amphibolite to greenschist facies) as well as ultramafic rocks, originally composed chiefly of harzburgite. Some of these associations favor the tectonism of a ridge-ridge transform system, but the evidence of island arc (or simply arc) and even off-ridge magmatism suggests that other processes were involved. The entire ophiolitic body may be the product of several magmatic and tectonic events, but in any case it was emplaced along the Trench landward slope area before the early Eocene. The tectonic history may be similar to that of the basalt-chert sequence in the Nicoya Peninsula, but further study is necessary before good understanding of this complex region can be attained.

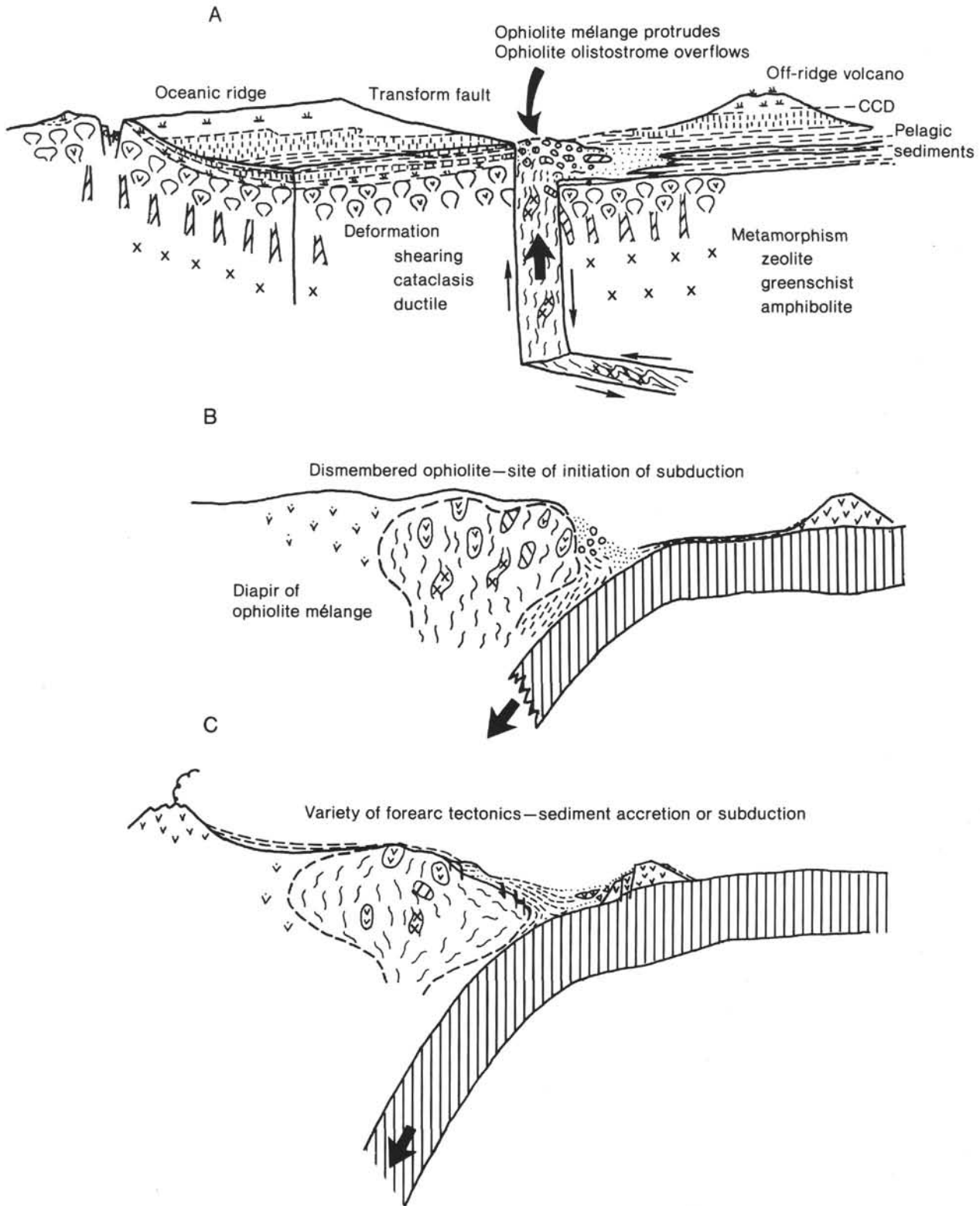


Figure 15. One of the possible modes of emplacement of dismembered ophiolitic rocks in forearc area (adapted after Ogawa and Naka, 1984). A. First ophiolite *mélange* is formed along a ridge-ridge transform fault, metamorphosed and deformed in a high geothermal gradient and under lateral shearing, then deformed by normal faulting in a nontransform segment of a fracture zone. An off-ridge volcano is possibly trapped in this zone. (After Karson and Dewey, 1978.) B. The buoyant ridge made up of such an ophiolite *mélange* becomes the site of the initiation of subduction, and the ophiolite *mélange* subsequently occupies the Trench landward area. C. Upheaval of the diapir may cause extensional deformation in the forearc region, where trench sediments are chiefly subducted, but the extent of the tectonics may vary because of other factors (Ogawa and Naka, 1984).

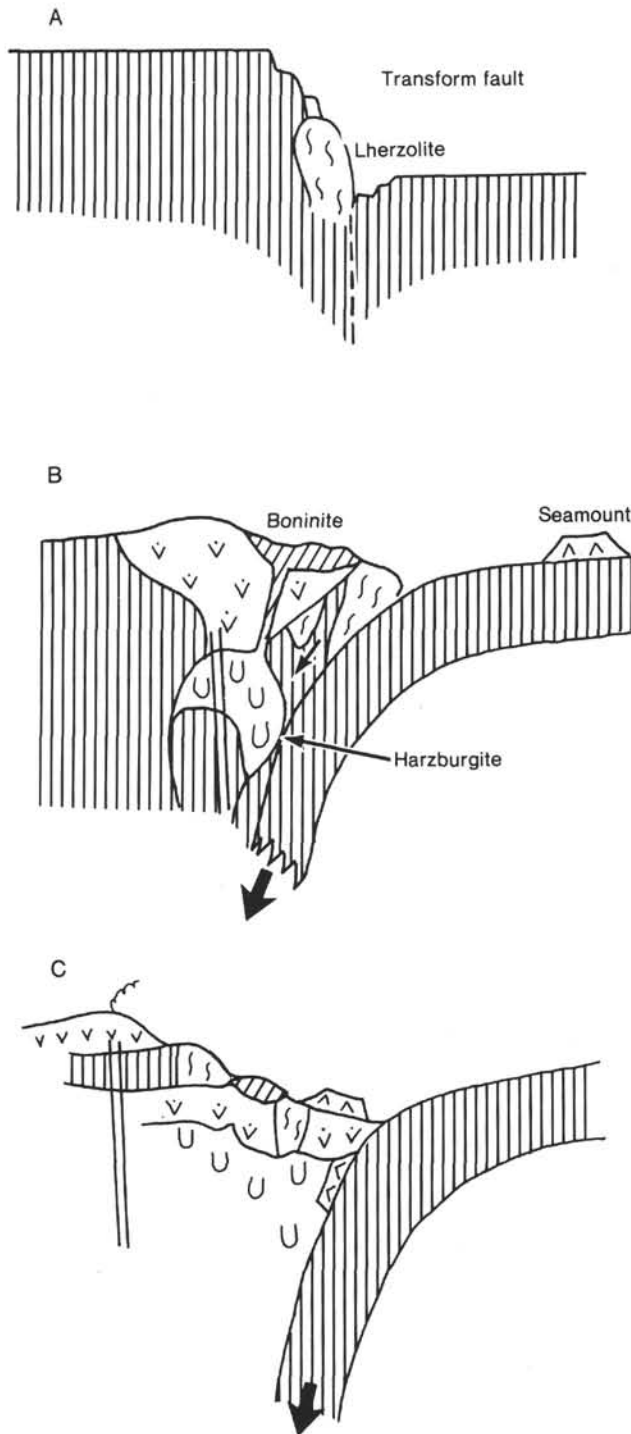


Figure 16. Alternative possible mode of emplacement of dismembered ophiolitic rocks in forearc area adapted and modified after Crawford et al. (1981) and Bloomer (1983). A. First subduction begins at a transform fault, where lherzolite (stretched s-shape) is emplaced and strong serpentinization occurs. B. Then arc lavas (dotted v-shape) and boninite (hachured) erupt and extremely depleted harzburgite (u-shape) is emplaced as the residue after boninite extraction (Crawford et al., 1981; Kushiro, 1983). C. Next, arc volcanic rocks erupt and a part of a seamount (reversed v-shape) is accreted; then the tectonic mixture of these rocks produces an ophiolitic mélange.

#### ACKNOWLEDGMENTS

We are grateful to Noriyuki Nasu, Kazuo Kobayashi, and Kame-toshi Kanmera for encouragement throughout the study. Technical assistance by Nicolas Royall, Grace Lau, and Richard Giddens at Imperial College is gratefully acknowledged. We also thank Harry Shaw, Robert Thompson, Ernest Rutter, Masayuki Komatsu, and Haruo Shirozu for valuable discussion. An early draft of the chapter was critically reviewed by Daniel E. Karig and J. Casey Moore, to whom we wish to express our gratitude.

#### REFERENCES

- Aubouin, J., von Huene, R., Azéma, J., Blackinton, G., Carter, J., Coulbourn, W., Cowan, D., Curiale, J., Dengo, C., Faas, R., Harrison, W., Hesse, R., Hussong, D., Ladd, J., Muzylov, N., Shiki, T., Thompson, P., and Westerberg, 1982. *Init. Repts. DSDP, 67*: Washington (U.S. Govt. Printing Office).
- Aubouin, J., von Huene, R., Baltuck, M., Arnott, R., Bourgois, J., Filwicz, M., Helm, R., Kvenvolden, K., Lienert, B., McDonald, T., McDougal, K., Ogawa, Y., Taylor, E., and Winsborough, B., 1982. Leg 84 of the Deep Sea Drilling Project. Subduction without accretion: Middle America Trench off Guatemala. *Nature*, 297: 458-460.
- Azéma, J., and Tournon, J., 1982. The Guatemala margin, the Nicoya Complex and the origin of the Caribbean Plate. In Aubouin, J., von Huene, R., et al., *Init. Repts. DSDP, 67*: Washington (U.S. Govt. Printing Office) 739-745.
- Bloomer, S. H., 1983. Distribution and origin of igneous rocks from the landward slopes of the Mariana trench: implications for its structure and evolution *J. Geophys. Res.*, 88: 7411-7428.
- Bloomer, S. H., and Hawkins, J. W., 1983. Gabbroic and ultramafic rock from the Mariana trench: an island arc ophiolite. In Hayes, D., (Ed.), *Tectonic and Geologic Evolution of Southeast Asia, Seas and Islands. Pt. 2*, AGU Monograph Ser. 27, pp 294-317.
- Bonatti, E., 1976. Serpentine protrusions in the oceanic crust. *Earth Planet. Sci. Lett.*, 32:107-113.
- Bonatti, E., and Hamlyn, P. R., 1981. Oceanic ultramafic rocks. In Emiliani, C., (Ed.), *The Sea*, (Vol. 7): New York (Wiley-Interscience), 241-283.
- Buckley, H. A., Bevan, J. C., Brown, K. M., and Johnson, L. R., 1978. Glauconite and celadonite: two separate mineral species. *Miner. Mag.*, 42:373-382.
- Casey, J. F., Dewy, J. F., Fox, P. J., Karson, J. A., and Rosencrants, E., 1981. Heterogeneous nature of oceanic crust and upper mantle: a perspective from the Bay of Islands ophiolite complex. In Emiliani, C. (Ed.), *The Sea*, (Vol. 7): New York (Wiley-Interscience), 305-338.
- Crawford, A. J., Beccaluva, L., and Serri, G., 1981. Tectono-magnetic evolution of the west Philippine-Mariana region and the origin of boninites. *Earth. Planet. Sci. Lett.* 54:346-356.
- Dietrich, V., Emmermann, R., Oberhänsli, R., and Puchelt, H., 1978. Geochemistry of basaltic and gabbro rocks from the west Mariana basin and the Mariana trench. *Earth. Planet. Sci. Lett.*, 39: 127-144.
- Fox, P. J., Schreiber, E., Rowlett, H., and McCamy, K., 1976. The geology of the Oceanographer fracture zone: a model for fracture zone. *J. Geophys. Res.*, 81:4117-4128.
- Francis, T. J. G., 1981. Serpentinization faults and their role in the tectonics of slow spreading ridges. *J. Geophys. Res.*, 86:11616-11622.
- Galli-Oliver, C., 1979. Ophiolite and island-arc volcanism in Costa Rica. *Geol. Soc. Am. Bull.*, 90:(Pt. I):444-452.
- Gass, I. C., and Smewing, J. D., 1981. Ophiolites: obducted oceanic lithosphere. In Emiliani, C. (Ed.), *The Sea*, (Vol. 7): New York (Wiley Interscience), 339-362.
- Gursky, H. -J., Schmidt-Effing, R., Strebin, M., and Wildberg, H., 1982. The ophiolite sequence in northwestern Costa Rica (Nicoya Complex): outlines of stratigraphical, geochemical, sedimentological and tectonical data. *Quinto Congreso Latinoamericano de Geología, Argentina, Actas*, 11:607-619.
- Humphries, S. E., Nelson, W. E., and Thompson, R. N., 1980. Basalt weathering on the East Pacific Rise and the Galapagos spreading center. In Rosendahl, B. R., Heikiniian, R., et al., *Init. Repts. DSDP, 54*: Washington (U.S. Govt. Printing Office), 773-787.

- Hussong, D. M., and Fryer, P., 1983. Fore-arc tectonics in the northern Mariana arc. In *Seminar on Formation of Ocean Margins*. Abs. Oji Internat., p. 32.
- Ishii, T., 1983. Origin of the Ogasawara fore-arc seamount or "Ogasawara Paleoland." In *Seminar on Formation of Ocean Margins*, Abs. Oji Internat., p. 91.
- Karson, J., and Dewey, J. F., 1978. Coastal complex, western Newfoundland: an early Ordovician oceanic fracture zone. *Geol. Soc. Am. Bull.*, 89:1037-1049.
- Kuijpers, E. P., 1980. The geologic history of the Nicoya ophiolite complex, Costa Rica, and its geotectonic significance. *Tectonophysics*, 68:233-255.
- Kushiro, I., 1983. Generation of magmas and upper mantle materials in Japanese Islands. In *Seminar on Formation of Ocean Margins*, Abs. Oji Internat., p. 44.
- Lundberg, N., and Moore, J. C., 1982. Evolution of the slope landward of the Middle America Trench, Nicoya Peninsula, Costa Rica. In Leggett, J. K. (Ed.), *Trench-Forearc Geology*. Geol. Soc. London Spec. Publ., 10:131-147.
- Miyashiro, A., 1973. The Troodos Ophiolite Complex was probably formed in an island arc. *Earth Planet. Sci. Lett.*, 19:218-224.
- Morrison, A. M., and Thompson, R. N., 1983. Alternation of basalt: Deep Sea Drilling Project, Legs 64 and 65. In Lewis, B. T. R., Robinson, P., et al., *Init. Repts. DSDP*, 65: Washington (U.S. Govt. Printing Office), 643-652.
- Nishiyama, T., 1979. Geological and petrological studies of the Nishisonogi metamorphic rocks (Master thesis). Kanazawa University.
- Ogawa, Y., 1983. Mineoka ophiolite belt in the Izu forearc area—Neogene accretion of oceanic and island arc assemblages in the northeastern corner of Philippine Sea Plate. In Hashimoto, M., and Uyeda, S. (Eds.), *Accretion Tectonics in Circum-Pacific Regions*: Tokyo, (Terra Sci. Pub.), pp. 235-250.
- Ogawa, Y., and Naka, J., 1984. Emplacement of ophiolitic rocks in forearc areas. In Gass, I. G., Lippard, S. J., and Shelton, A. W. (Eds.), *Ophiolites and Ocean Lithosphere*. Geol. Soc. London Spec. Publ., 13:91-301.
- Robertson, A. H. F., and Hudson, J. D., 1973. Cyprus umbers: chemical precipitates in a Tethyan ocean ridge. *Earth Planet. Sci. Lett.*, 18:93-101.
- Rutter, E., Peach, C. J., White, S. H., and Johnson, D., 1982. Experimental deformation of basalt under conditions of syntectonic hydration. In *Conf. on Planar and Linear Fabric of Deformed Rocks, Zurich*, Abs. Internat., pp. 249-252.
- Schmidt-Effing, R., 1979. Alter und Genese des Nicoya-Komplexes, ein ozeanischer Paläokurste (Oberjura bis Eozän) im südlichen Zentralamerika. *Geol. Rundsch.*, 68:457-494.
- Seely, D. R., 1979. The revolution of structural highs bordering major forearc basins. *Am. Assoc. Petrol. Geol. Mem.*, 29:245-260.
- von Huene, R., Aubouin, J., Azéma, J., Blackinton, G., Carter, J., Coulbourn, W., Cowan, D., Curiale, J., Dengo, C., Faas, R., Harrison, W., Hesse, R., Hussong, D., Ladd, J., Muzylov, N., Shiki, T., Thompson, P., and Westerberg, J., 1980. Leg 67: the Deep Sea Drilling Project Mid-America Trench transect off Guatemala. *Geol. Soc. Am. Bull.*, 91 (Pt. I): 421-432.

Date of Initial Receipt: 10 August 1983

Date of Acceptance: 6 February 1984